Fracture of random central force networks under tension: the stretched net model of the erythrocyte membrane skeleton



1993 J. Phys.: Condens. Matter 5 4749

(http://iopscience.iop.org/0953-8984/5/27/019)

J. Phys.: Condens. Matter 5 (1993) 4749–4758. Printed in the UK

# Fracture of random central force networks under tension: the stretched net model of the erythrocyte membrane skeleton

Malcolm J Grimson

Theory and Computational Science Group, AFRC Institute of Food Research, Norwich Laboratory, Norwich Research Park, Colney, Norwich NR4 7UA, UK

Received 14 December 1992, in final form 5 April 1993

**Abstract.** A random central force network model of the erythrocyte membrane skeleton is constructed by the relaxation of a bond diluted triangular lattice of Hooke's law springs under tension. The fracture of such a network is studied numerically by including a maximum value, $L_b$, for the extension of any spring before irreversible breakage. The model shows a mechanical instability for values of $L_b$ less than a well defined critical value at any bond fraction above the percolation threshold. For undeformed networks that are mechanically stable, the fracture characteristics under an applied strain can be quantified as a function of $L_b$, the bond fraction and the type of sample deformation.

## 1. Introduction

The erythrocyte membrane skeleton is a network of structural proteins attached to the cytoplasmic surface of the plasma membrane. This network restricts the lateral diffusion of membrane proteins and provides mechanical reinforcement to the membrane of the erythrocyte. The structure of the erythrocyte membrane skeleton has been reviewed by Palek and Lambert [1]. The principal structural proteins in the skeleton responsible for its mechanical rigidity are spectrin and actin. Spectrin is a flexible, rod-shaped protein comprising two subunits which associate side-to-side to form a heterodimer. The heterodimers associate head-to-head into tetramers which form the bonds of a network. Actin oligomers form the nodes of the network, binding typically six tetramers by the tail. The network structure is, on average, well represented by a triangular lattice [2]. Defects in the membrane skeleton result in spectrin-free regions of the network which can significantly alter the mobility of proteins within the membrane as well as the mechanical properties of the erythrocyte.

Saxton [3] introduced a simple random central force network model of the erythrocyte membrane skeleton generated by the random bond dilution of a triangular lattice of Hooke's law springs under tension and studied the geometrical properties of the network, in particular the distribution of pore sizes. The model was based on the stretched spring net of Tang and Thorpe [4] who have presented a systematic study of the linear elastic properties of the elastically isotropic system as a function of the bond fraction. Experiments have measured the shear modulus of the erythrocyte membrane [5, 6] and show a temperature dependence consistent with a model comprising a random network of stretched springs. However the correspondence of the stretched net model to the erythrocyte membrane skeleton, in regard to the elastic behaviour under large deformations and the mechanisms leading to fracture, is less clear.

0953-8984/93/274749+10$07.50  

The fracture failure of random networks, being a dynamical process, is an inherently more difficult process to study and simulate than elasticity. Nevertheless, several authors have made studies of some aspects of the fracture of central force networks of harmonic springs under an applied stress or strain. Ashurst and Hoover [7] investigated the fracture of a two-dimensional triangular lattice of identical particles interacting through a truncated Hooke's law force by molecular dynamics, while Beale and Srolovitz [8], Hansen, Roux and Herrmann [9] and Sahimi and Goddard [10] have all used Monte Carlo methods to study the rupture of two dimensional lattices of springs with three general classes of disorder: (i) random bond deletion, (ii) randomly distributed spring fracture lengths and (iii) randomly distributed spring force constants. These studies have shown the fracture process to be a complex interplay of the quenched disorder in the system and the redistribution of local stresses in the network as the fracture proceeds by the formation and growth of cracks.

In general, the growth of cracks in a disordered system is a non-linear, non-equilibrium phenomenon which does not usually occur at random, but is dependent upon the stress or strain field around the cracks. In contrast the static and linear elastic properties of disordered systems are usually modelled by percolation networks in which the bonds are cut at random [11]. Under certain conditions the accumulation of damage and growth of cracks could take place essentially at random and a percolation process would then describe the fracture phenomena. Indeed it has been argued [10, 12] that in the limit of infinite disorder of the spring fracture threshold, the fracture of central force networks is equivalent to a percolation process. However, in real materials and most discrete models of mechanical breakdown disorder is finite and thus fractured and percolation networks differ.

The similarities and differences between fracture and percolation processes have been investigated by Sahimi and Arbabi for percolation networks with central and bond-bending forces [13, 14]. For systems which are macroscopically homogeneous, regardless of the form of the disorder distribution, the initial stages of both fracture and percolation processes are very similar with bonds that are broken according to any failure criterion being distributed essentially at random throughout the network. In these initial stages, stress enhancement at the tip of a microcrack is insufficient to ensure that the next bond to break will be at the tip of the microcrack. However, as microcracks nucleate the effect of stress enhancement increases and beyond a certain point (typically around the maximum in the stress–strain curve) there will be no similarity between fracture and percolation processes.

In regard to the fracture failure of randomly diluted central force networks under tension, only for networks which are in the limit of small disorder or near a percolation threshold is the situation somewhat clarified. Saxton's stretched spring network model of the erythrocyte membrane skeleton constitutes an example of a system in the intermediate regime, where there is a strong short-range ordering of the bonds but long-range disorder. The short-range bond correlations can be expected to have a major influence on both the fracture mechanism and the stress–strain curve. In this paper the fracture of two-dimensional bond diluted triangular networks under tension is investigated by assigning a single load limit to the network springs which irreversibly break if the spring is extended beyond a critical length using an energy minimization method. A description of the model and the simulation method is given in the following section. In section 3 the mechanical stability of undeformed network is investigated to determine the range of parameters over which a macroscopic stress or strain can be applied to the network. The fracture characteristics of the model network under applied strains is studied in section 4 and the paper concludes with a discussion of the results.

## 2. Model and simulation method

An elastic network is constructed from a lattice where all the bonds between nearest-neighbour sites are Hooke's law springs. The sites of the initial lattice define the nodes of the elastic network. The Hooke's law spring connecting nodes $i$ and $j$, located at $\boldsymbol{r}_i$ and $\boldsymbol{r}_j$ respectively, is characterized by a force constant $K$, a natural (unstretched) length of zero and a fracture length $L_b$. The elastic potential energy for this model is given by [4]

$$E = \tfrac{1}{2}\sum_{i<j}{}' K_{ij}(|\boldsymbol{r}_i - \boldsymbol{r}_j|)^2 \tag{1}$$

where the prime denotes that the summation is only over nearest-neighbour bonds and $K_{ij} = K$ or 0 depending upon whether the bond is present or absent. The force $\boldsymbol{F}_i$ on $i$th node of the network is given by

$$\boldsymbol{F}_i = -\partial E/\partial \boldsymbol{r}_i = \sum_j{}' K_{ij}|\boldsymbol{r}_i - \boldsymbol{r}_j|\hat{\boldsymbol{r}}_{ij} \tag{2}$$

where $\hat{\boldsymbol{r}}_{ij} = (\boldsymbol{r}_j - \boldsymbol{r}_i)/|\boldsymbol{r}_i - \boldsymbol{r}_j|$ is the unit vector between nodes $i$ and $j$. The equilibrium condition for the network is that the total force acting on each node of the network must vanish, namely

$$\boldsymbol{F}_i = -\partial E/\partial \boldsymbol{r}_i = 0 \tag{3}$$

for all $i$. For an undiluted network, the sites of the lattice will correspond to equilibrium positions of the network nodes since the forces exerted on each site by the stretched springs balance each other. However, following bond dilution of the lattice, this force balance is destroyed and the network must deform so as to move the nodes of the network to their equilibrium positions which may be far away from the corresponding original lattice sites.

In this paper a diluted lattice is generated by randomly removing bonds from a two-dimensional triangular lattice. The resulting random network is relaxed to equilibrium by solving purely dissipative equations of motion for the nodes of the network given by [15]

$$\eta \mathrm{d}\boldsymbol{r}_i/\mathrm{d}t = -\partial E/\partial \boldsymbol{r}_i \tag{4}$$

for all $i$, where $\eta$ is a fraction coefficient. During the relaxation if any bond is stretched to a length greater than the spring fracture length $L_b$ it is irreversibly broken. Thus for sufficiently small values of $L_b$ there will be a decrease in the number of bonds in the system during the relaxation to equilibrium. The bond fraction of the system is given by

$$p = (1/2N_n)\sum_{i,j}{}' (K_{ij}/K) \tag{5}$$

where $N_n$ is the number of nodes in the system. If $p_0$ denotes the initial bond fraction of the system prior to relaxation, then in equilibrated networks $p \leqslant p_0$.

The coupled equations of motion for the nodes of (2) and (4) are solved numerically using the Euler method [16]. Specifically, during the iteration procedure, the position of node $i$ is determined from the previous configuration by

$$\boldsymbol{r}_i^{(n+1)} = \boldsymbol{r}_i^{(n)} + \alpha \boldsymbol{F}_i^{(n)} \tag{7}$$

where the parameter $\alpha = \Delta t/\eta$ (or the time step $\Delta t$) is adjusted to ensure the convergence of the iteration. The time step should not be too large, since at each step in the iteration bonds whose length exceeds $L_b$ must be irreversibly broken. Typically a value of $\alpha \leqslant 0.1$ was used in this work. The iteration process should stop when the force on every node of the network is zero. However, in practice, an appropriate small value for the force on any node, $|F_m|$, is chosen that is good enough to give the final precision required. Thus the relaxation procedure is terminated when $|F_i| < |F_m|$ for all $i$. The elastic energy per unit area of the equilibrium two-dimensional network is denoted $E_0$ and the tension $T$ is determined from the force per unit length perpendicular to an imaginary line through the network.

In this paper an initial triangular lattice comprising $N_n$ nodes was embedded in a simulation cell of size $L_x \times L_y$ with periodic boundary conditions to maintain the network tension [4]. The nearest-neighbour lattice spacing defines the unit of length and restricts the range of physical values for spring fracture length in this model to $L_b > 1$. The force constant of the spring sets the energy scale of the model. A maximum force on any node of $|F_m|/K = 10^{-3}$ was used to terminate the relaxation procedure. This typically corresponded to errors in $E_0/K$ for the equilibrated network of order $10^{-8}$. Such a choice leads to errors in the calculated elastic properties of equilibrium networks prior to fracture which are less than the statistical uncertainty.

The fracture of the random network under tension was simulated by applying a series of small uniform strains of magnitude $\epsilon$ to the sample. Following each application of the strain, the deformed network was relaxed back to equilibrium and the $x$ component of the tension, $T_x$, in the network calculated. If the network had fractured, i.e. $T_x = 0$, the sequence of deformations was terminated. Otherwise additional cycles of deformation and relaxation were applied until fracture of the sample occurred. Three different types of strain deformation were considered:

(a) uniaxial extension in the $x$-direction, in which the system was deformed according to

$$x^* = (1+\epsilon)x \text{ and } y^* = y \tag{7}$$

(b) uniform expansion when

$$x^* = (1+\epsilon)x \text{ and } y^* = (1+\epsilon)y \tag{8}$$

(c) compression/expansion at constant sample area in which

$$x^* = (1+\epsilon)x \text{ and } y^* = y/(1+\epsilon) \tag{9}$$

where the asterisk denotes coordinates in the deformed system.

Thus for $\epsilon > 0$, the sample undergoes a series of elongational deformations in the $x$-direction with the elongation of the sample in the $x$-direction being given by

$$(L_x^* - L_x)/L_x = L_x^*/L_x - 1 = (1+\epsilon)^N \tag{10}$$

where $N$ is the number of strain cycles applied. Note that the deformations (b) and (c) of uniform expansion and compression–expansion are identical to those used to determine the two independent linear elastic moduli in the small deformation limit [16].

The results presented here were averaged over ten random initial configurations for each set of parameter values with $N_n = 1968$, $L_x = 41$ and $L_y = 24\sqrt{3}$. The finite size scaling of the linear elastic and fracture properties has been studied by Sahimi and Arbabi [14] who investigated percolation networks with central and bond-bending forces in both two and three dimensions.

## 3. Mechanical stability of the undeformed network

The mechanical stability of the undeformed networks was first investigated and figure 1 shows the elastic energy per unit area $\langle E_0 \rangle$ of the equlibrium network, which Tang and Thorpe [4] have shown to be identical to the isotropic network tension $\langle T \rangle$, as a function of $L_b$ for a number of values of the initial bond fraction $p_0$ above the percolation threshold $p_c = 0.347$ [14]. First note that the qualitative features of the results are the same for all values of $p_0$ with $\langle E_0 \rangle$ showing a distinctive sharp reduction from a constant value to zero, corresponding to sample fracture, as a function of decreasing $L_b$. For any value of $p_0$ there clearly exists a critical value of $L_b$ above which $\langle E_0 \rangle$ is independent of $L_b$ and has a value equal to that obtained for $L_b \to \infty$. For values of $L_b$ lower than this critical value, $\langle E_0 \rangle$ is a monotonic decreasing function of $L_b$.

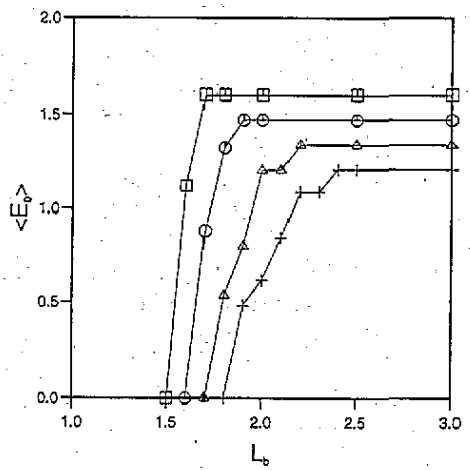


**Figure 1.** Elastic energy per unit area $\langle E_0 \rangle$ (in units of $K$) as a function of the spring fracture length $L_b$ for different values of the initial bond fraction: $p_0 = 0.8$ (+), $p_0 = 0.85$ (△), $p_0 = 0.9$ (○) and $p_0 = 0.95$ (□).

The drop in the equilibrium energy per unit area with the onset of sample fracture is associated with a reduction in the number of bonds in the simulation cell due to their irreversible breakage during relaxation and indeed the mean bond fraction is a monotonic decreasing function of $L_b$ once the critical value of $L_b$ is passed. However, in contrast to the large fall seen in $\langle E_0 \rangle$, over the same range of $L_b$ values there is only a small decrease in $\langle p \rangle$. If the bond fraction at sample fracture is denoted $p_f$, then a plot of $\langle p_f \rangle$ against $p_0$ for the undeformed network displays a linear relationship with $\langle p_f \rangle = 0.07 + 0.88\ p_0$ for $0.55 \leqslant p_0 \leqslant 0.95$. Thus the mean bond fraction at sample fracture $\langle p_f \rangle$ is well above $p_c$ for the range of $p_0$ considered here. Since not many bonds are broken during relaxation, the dramatic change in $\langle E_0 \rangle$ occurring with the onset of sample fracture is the result of a significant alteration to the equilibrium bond length distribution. Thus the mechanical stability of the network is seen to be controlled by a relatively small number of highly stretched bonds in the network, whose breakage leads to mechanical failure of the sample. These findings are consistent with the behaviour seen in the fracture of three-dimensional random central force network models of gels [17].

From the definition of the model, for $p_0 = 1$ the critical value of $L_b$ corresponding to the onset of fracture is unity. Furthermore for $p_0 \to p_c$ the critical value of $L_b$ corresponding

to fracture tends to infinity. Thus interest focuses on the intermediate range of $p_c < p_0 < 1$. Figure 1 shows that for values of $p_0$ close to unity, the fracture transition is sharp, almost discontinuous, with a critical value for $L_b$ corresponding to fracture also close to unity. For example, at $p_0 = 0.95$ the critical value of $L_b$ corresponding to the onset of fracture is $L_b \simeq 1.7$. But as $p_0$ is reduced the spring fracture length corresponding to the onset of sample fracture is seen to shift to larger values and the transition region becomes much more rounded and extended. The rounding of the transition is a result of finite size effects [14], since the sample fracture is associated with the breakage of only a small number of bonds.

## 4. Fracture under applied strain

Above it was shown that for $p_0 > p_c$ the undeformed network is mechanically stable for a sufficiently large value of $L_b$ and a deformational strain can be applied. In this paper three different types of applied strain are considered: uniaxial extension, uniform expansion and compression/expansion. Figure 2 shows the characteristic stress–strain curves, namely the $x$ component of the tension $\langle T_x \rangle$ as a function of the sample elongation $(L_x^*/L_x - 1)$, for the three deformational strain types applied to networks under tension at an initial bond dilution of $p_0 = 0.9$ and a spring fracture length of $L_b = 2.5$. In addition figure 3 shows the dependence of the mean bond fraction $\langle p \rangle$ on the sample elongation $(L_x^*/L_x - 1)$ for the stress–strain curves of figure 2. In all of the three cases considered, for sample elongations up to the onset of fracture, $\langle T_x \rangle$ is non-decreasing and the mean bond fraction is constant with $\langle p \rangle = p_0$. Furthermore the system is reversible in the sense that the sign of the elongational strain may be reversed to recover the original undeformed network; but for greater sample elongations, $\langle T_x \rangle$ and $\langle p \rangle$ are reduced as bonds are irreversibly broken during relaxation and the original undeformed network cannot be recovered by reversing the applied strain.

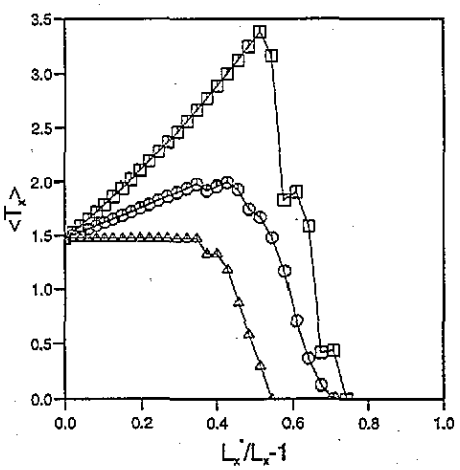


**Figure 2.** $x$ component of the tension $\langle T_x \rangle$ (in units of $K$) as a function of the sample elongation in the $x$ direction $L_x^*/L_x - 1$ for initial bond fraction $p_0 = 0.9$, spring fraction $L_b = 2.5$ and three different forms of applied strain: compression/expansion (□), uniaxial extension (○) and uniform expansion (△).

Since the act of uniform expansion does not alter any of the relative locations of the nodes in an equilibrated network unless a bond is broken, fracture under uniform expansion is intimately related to the spontaneous mechanical instability of the undeformed network studied in the previous section. Thus from figure 1 it is known that for $L_b = 2.5$ the network will only be able to support any uniform expansion for $p_0 > 0.8$. For the case of uniform expansion with $p_0 = 0.9$ and $L_b = 2.5$ shown in figure 2, $\langle T_x \rangle$ is seen to be independent, within statistical error, of the sample elongation until the onset of fracture at $(L_x^*/L_x - 1) \simeq 0.36$. Thus prior to fracture the increase in the stored elastic energy of the system is compensated by the increase in the area of the simulation cell resulting from uniform expansion.

Next consider the average stress–strain curves for compression/expansion and uniaxial extension. Figure 2 shows that both types of deformation show a monotonic increase in $\langle T_x \rangle$ with sample elongation prior to onset of fracture after which any increased elongation leads to a dramatic and irreversible decrease in $\langle T_x \rangle$ associated with a small decrease in the mean bond fraction. Compression/expansion and uniaxial extension differ from uniform expansion in that deformation of the sample leads to a reorganization in the location of the nodes within the sample without any irreversible breakage of bonds. This reorganization of the network under deformation allows it to support greater applied strains prior to fracture. The stress-strain curve for uniaxial extension shows a linear dependence of $\langle T_x \rangle$ on the sample elongation up to a maximum value for the $x$ component of the tension, $\langle T_x \rangle_{max}$. For the case $L_b = 2.5$ and $p_0 = 0.9$ figure 2 shows $\langle T_x \rangle_{max} \simeq 2.0$ for uniaxial extension which corresponds to a sample elongation of $(L_x^*/L_x - 1) \simeq 0.4$. By way of contrast, for compression/expansion deformations the stress–strain curve is concave prior to the onset of fracture and so for any given sample elongation $\langle T_x \rangle$ must be greater for compression/expansion than for uniaxial strain. Furthermore the maximum sample elongation prior to the onset of fracture is also greater for compression/expansion than for uniaxial extension. The average strain–stress curve for compression/expansion of a network with $L_b = 2.5$ and $p_0 = 0.9$ in figure 2 shows a maximum at a sample elongation of $(L_x^*/L_x - 1) \simeq 0.5$ with $\langle T_x \rangle_{max} \simeq 3.44$.

Figure 3 shows that for all three types of sample deformation $\langle p \rangle$ is a monotonic decreasing function of the sample elongation from the elongation corresponding to $\langle T_x \rangle_{max}$ to that corresponding to fracture. Note that $\langle p_f \rangle$ is significantly smaller for the case of uniform expansion than for either compression/expansion or uniaxial extension, although in all three cases $\langle p_f \rangle \gg p_c$. Thus sample fracture under applied strain is also seen to be the result of crack growth and is not a percolation process.

For all three types of deformation, the principal role of the spring fracture length is to control the maximum sample elongation prior to fracture. By way of example, the $L_b$ dependence of the stress–strain curve for a network with $p_0 = 0.9$ subject to uniaxial strain is shown in figure 4 with the corresponding dependence of the mean bond fraction on the sample deformation shown in figure 5. From figure 4 it is immediately apparent that the shape of the stress–strain curve is essentially independent of $L_b$ for all values of $L_b$ greater than that required for mechanical stability of the undeformed network. For the case shown in figure 4 of uniaxial strain applied to a network with $p_0 = 0.9$, this requires $L_b > 1.8$. $\langle T_x \rangle_{max}$ and the sample elongation corresponding to $\langle T_x \rangle_{max}$ are both approximately linear increasing functions of $L_b$. For $L_b > 2.0$ the shape of the curves plotting the mean bond fraction against sample deformation are also essentially independent of $L_b$. The sample elongation corresponding to the initial breakage of bonds is an approximately linear increasing function of $L_b$. Only as $L_b$ is reduced toward the value at which the system is unable to support any deformation without bond fracture during relaxation is there a small

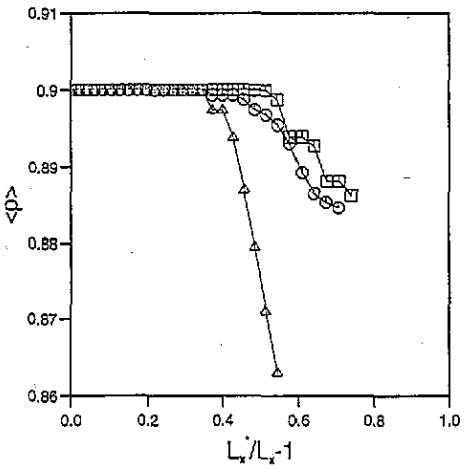


**Figure 3.** Bond fraction $\langle p \rangle$ as a function of the sample elongation in the $x$ direction $L_x^*/L_x - 1$ for initial bond fraction $p_0 = 0.9$, spring fraction $L_b = 2.5$ and three different forms of applied strain: compression/expansion (□), uniaxial extension (○) and uniform expansion (△).

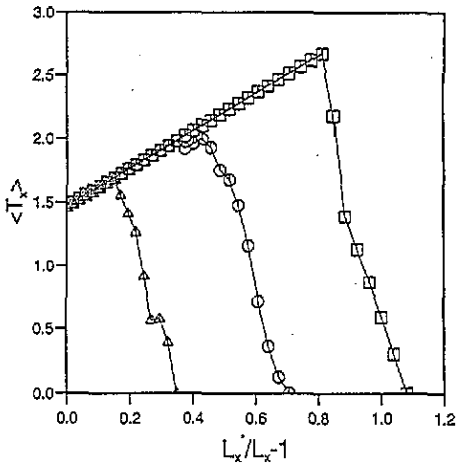


**Figure 4.** $x$ component of the tension $\langle T_x \rangle$ (in units of $K$) as a function of the sample elongation $L_x^*/L_x - 1$ for a network under uniaxial strain with initial bond fraction $p_0 = 0.9$ and three different values of the spring fracture length: $L_b = 2.0$ (△), $L_b = 2.5$ (○) and $L_b = 3.0$ (□).

change in the shape of the mean bond fraction against sample elongation curve.

As the initial bond fraction of the network is reduced for a given spring fracture length, the maximum sample elongation prior to the onset of sample fracture is reduced until the undeformed network is no longer mechanically stable. Figure 6 shows the dependence of the average stress–strain curve upon the initial bond fraction for a network with spring fracture length $L_b = 2.5$ under uniaxial extension. The sample elongation corresponding to $\langle T_x \rangle_{max}$ is seen to be an approximately linear increasing function of $p_0$ for $p_0 \geqslant 0.65$, while for $p_0 < 0.65$ the network is unable to support any uniaxial extension without the irreversible breakage of bonds. If the mean bond fraction at fracture $\langle p_f \rangle$ is plotted against the initial bond fraction $p_0$ for the case shown in figure 6 of the uniaxial extension of a network with $L_b = 2.5$, a linear relationship with $\langle p_f \rangle = 0.02 + 0.95\ p_0$ is seen to hold over the range $0.55 \leqslant p_0 \leqslant 0.95$. Thus $\langle p_f \rangle$ is greater than the percolation threshold $p_c$ and fracture under applied strain within this model does not correlate with the onset of a percolation threshold, but is the result of crack formation and growth. Similar behaviour is observed for compression/expansion deformations.

For $L_b = 2.5$, figure 1 shows that under uniform expansion the network will not support any deformation prior to fracture for $p_0 < 0.8$. For $p_0 \geqslant 0.8$ however, the sample elongation which the network will support prior to fracture is again an approximately linear function of $p_0$. Thus there are a range of initial bond fractions for which networks will reversibly support uniaxial extension and compression/expansion deformations, but will not support any uniform expansion without the irreversible fracture of some network bonds.

## 5. Discussion

By introducing a fracture length to the network springs, which can irreversibly change the network topology during the relaxation to equilibrium, it has been shown that the fracture

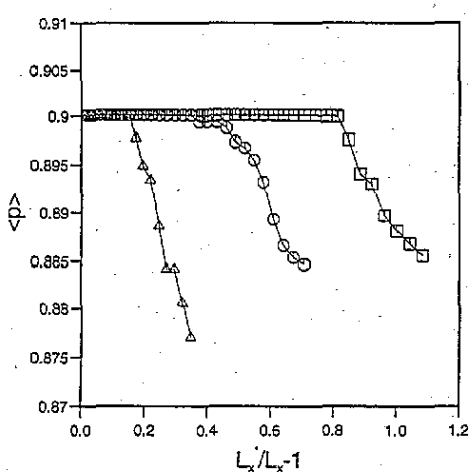


**Figure 5.** Bond fraction $\langle p \rangle$ as a function of the sample elongation $L_x^*/L_x - 1$ for a network under uniaxial strain with initial bond fraction $p_0 = 0.9$ and three different values of the spring fracture length: $L_b = 2.0$ (△), $L_b = 2.5$ (○) and $L_b = 3.0$ (□).

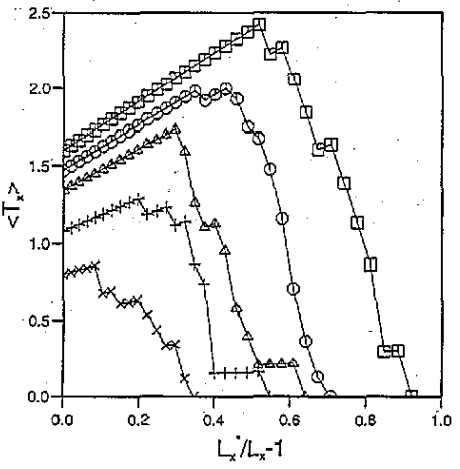


**Figure 6.** $x$ component of the tension $\langle T_x \rangle$ (in units of $K$) as a function of the sample elongation $L_x^*/L_x - 1$ for a network under uniaxial strain with spring fracture length $L_b = 2.5$ and five different values of the initial bond fraction: $p_0 = 0.65$ (×), $p_0 = 0.75$ (+), $p_0 = 0.85$ (△), $p_0 = 0.9$ (○) and $p_0 = 0.95$ (□).

of a random central force network under tension can be quantified as a function of the initial bond fraction and the form of the applied strain. Fracture of the model network under a uniform external load for $p_0 > p_c$ is a result of the growth of cracks within the sample which depends upon the local environment and hence differs from a percolation process. The model clearly shows that a reduction of the bond fraction enhances the likelihood of rupture and thus correlates well with the behaviour expected of an erythrocyte membrane skeleton. However it should be noted that for any given value of the spring fracture length, the bond fraction at which the network is unstable to deformation is greater for uniform expansion than for uniaxial extension or compression/expansion types of deformation. Thus mechanical stability criteria for the erythrocyte membrane skeleton within this extension of the Saxton [3] model will depend upon the form of the applied strain with the model being least stable to uniform expansion.

Finally note that the stretched spring model presented here is of restricted validity, since the use of only central forces between nodes restricts attention to networks in which there is no direct interaction between the bonds of the network. Further extensions of Saxton's random network model of the erythrocyte membrane skeleton will require the introduction of non-central forces between nodes of the network to model the bond–bond interactions.

## References

[1] Palek J and Lambert S 1990 *Semin. Hematol.* **27** 290
[2] Liu S C, Derick L H and Palek J 1987 *J. Cell Biol.* **104** 527
[3] Saxton M J 1992 *J. Theor. Biol.* **155** 517
[4] Tang W and Thorpe M F 1987 *Phys. Rev.* B **36** 3798
[5] Waugh R and Evans E 1979 *Biophys. J.* **26** 115
[6] Engelhardt H and Sackmann E 1988 *Biophys. J.* **54** 495
[7] Ashurst W T and Hoover W G 1976 *Phys. Rev.* B **14** 1465
[8] Beale P D and Srolovitz D J 1988 *Phys. Rev.* B **37** 5500

[9] Hansen A, Roux S and Herrmann H J 1989 *J. Physique* **50** 733
[10] Sahimi M and Goddard J D 1986 *Phys. Rev.* B **33** 7848
[11] Stauffer D 1985 *Introduction to Percolation Theory* (London: Taylor and Francis)
[12] Roux S, Hansen A, Herrmann H J and Guyon E 1988 *J. Stat. Phys.* **52** 237
[13] Sahimi M and Arbabi S 1992 *Phys. Rev. Lett.* **68** 608
[14] Sahimi M and Arbabi S 1993 *Phys. Rev.* B **47** 695, 703, 713
[15] Nagai T, Kawasaki K and Nakamura K 1988 *J. Phys. Soc. Japan* **57** 2221
[16] Tang W and Thorpe M F 1988 *Phys. Rev.* B **37** 5539
[17] Grimson M J 1992 *Mol. Phys.* **76** 1375